

# CONGRUENT MELTING OF BINARY COMPOUNDS WITH NON-NEGLIGIBLE VAPOUR PRESSURE

## II. Application to the sulfaguanidine–water system

J. C. Rouland, S. Makki\*, J. L. Fournival\*\* and R. Céolin\*\*

Laboratoire de Chimie Physique, Faculté de Médecine et de Pharmacie, Place Saint-Jacques, F25030 Besançon Cedex, France

\*Laboratoire de Pharmacie Galénique, Faculté de Médecine et de Pharmacie, Place Saint-Jacques, F25030 Besançon Cedex, France

\*\*Laboratoire de Chimie Physique, Faculté de Pharmacie, 2bis, Bd Tonnelé, F37042 Tours Cedex, France

### Abstract

The sulfaguanidine–water (*SG*-H<sub>2</sub>O) system is a binary system with non-negligible vapour pressure which presents a monohydrate. The phase diagram of this system is drawn from DTA experimental results, using the temperature-specific volume-molar fraction ( $T$ - $v$ - $x$ ) model which was described in part I of this work.

The melting of the monohydrate (*SG*, H<sub>2</sub>O) is found to be congruent. Isochoric sections are drawn; they make it possible to determine the limits of the two eutectic invariant planes. The composition and specific volume of the vapour phase at the eutectic equilibrium of the *SG*-*SG*, H<sub>2</sub>O subsystem are given. The triple line solid-liquid-vapour of the one-component phase diagram of the monohydrate is drawn. The experimental results are consistent with the congruent melting of the monohydrate. These results also show that the solid, liquid and vapour phase at the triple line have not the same composition.

**Keywords:** congruent melting, sulfaguanidine–water system

### Introduction

In this paper, the sulfaguanidine–water system is presented as an illustration of a theory of congruent melting of binary compounds, which we have dealt with in our previous paper [1].

Sulfaguanidine (C<sub>7</sub>H<sub>10</sub>N<sub>4</sub>O<sub>2</sub>S) is an antibacterian sulphamide, used for intestinal infections. Two anhydrous forms of sulfaguanidine (*SG*) and one monohydrate form (*SG*, H<sub>2</sub>O) may be obtained. The structural study has been achieved by Alberola *et al.* [2]. In the present work we have employed two forms which have been identified by comparing the X-ray patterns which we obtained to the lattice parameters given by these authors (Table 1).

**Table 1** Sulfaguanidine crystallographic data after Alberola *et al.*

	Anhydrous form (form I)	Monohydrate
<i>M</i>	214.26	232.26
a (Å)	10.414(6)	7.536(3)
b (Å)	20.219(20)	5.450(4)
c (Å)	7.037(6)	24.593(15)
α (°)	82.86(6)	90.00
β (°)	95.29(5)	90.34(5)
γ (°)	95.93(4)	90.00
volume (Å <sup>3</sup> )	1451.398	1012.889
<i>Z</i>	6	4
<i>m/V</i> calc. (mg·mm <sup>-3</sup> )	1.49	1.52
<i>V/m</i> (mm <sup>-3</sup> ·mg <sup>-1</sup> )	0.671	0.658

## Study of the monohydrate

Thermogravimetric analysis (TG) and Differential Thermal Analysis (DTA) in open vessels were performed on a DuPont 990 thermal analyser.

### a) Thermogravimetric analysis (TG)

Thermogravimetric analysis (Fig. 1) shows that the sulfaguanidine hydrate starts losing its hydration water at a temperature which is far from the melting point. Almost all the water is lost before the starting of the melting. Therefore, this form can be considered as a hydrate with a non negligible vapour pressure. It has also been possible to check, by TG, the stoichiometric composition of this compound: one mole water for one mole anhydrous compound.

### b) Differential thermal analysis (DTA) in open vessels

The DTA curve (Fig. 1) shows a first endotherm (a) which starts at 80°C. It relates the almost total loss of water:



It is followed by a second endotherm (b) at 140°C which corresponds to the eutectic equilibrium between the hydrate form (SG, H<sub>2</sub>O) which has not yet completely disappeared, the anhydrous form (SG) and the liquid. It is followed

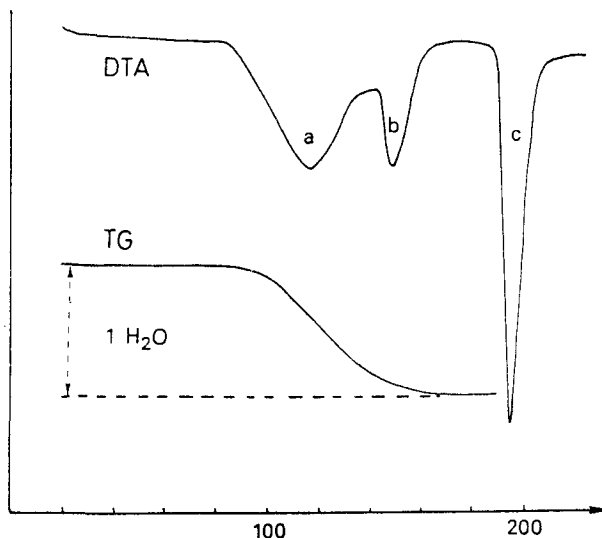


Fig. 1 DTA and TG curves of the sulfaguandine monohydrate in open vessels (heat rate: 10 deg·min<sup>-1</sup>)

by the endotherm c which corresponds to the melting of the anhydrous compound SG. The hydrate has disappeared.

It can be noticed that, in a previous work, the same DTA and TG curves have been observed for another hydrate: phenanthroline-1,10 monohydrate [3].

### c) Differential thermal analysis in closed vessels

The hydrate compound has been analysed, with the MCB ARION microcalorimeter, in sealed pyrex vessels in order to reduce the dissociation of the hydrate form. In this case, the DTA curve is quite different from the previous one (Fig. 2).

For a low value of the massic volume  $V/m \approx 4 \text{ mm}^3 \cdot \text{mg}^{-1}$  (where  $V$  is the internal volume of the vessel and  $m$  is the total mass of the sample), only one peak has been observed. This peak can be related to the presence of a second phase: the liquid phase. It is important to point out that this peak starts more progressively, compared to the peak obtained for the melting point of the anhydrous compound (Fig. 1, peak c): it looks like a liquidus peak. Nevertheless, this shape cannot be due to impurities. The effect of impurities should be the same for the two peaks since both hydrate and anhydrous compounds are obtained from the same sample.

Two phenomenons occurred

1) In the sealed tube containing hydrate, there was a non negligible dead volume. When the hydrate of sulfaguandine was introduced in the tube, equilib-

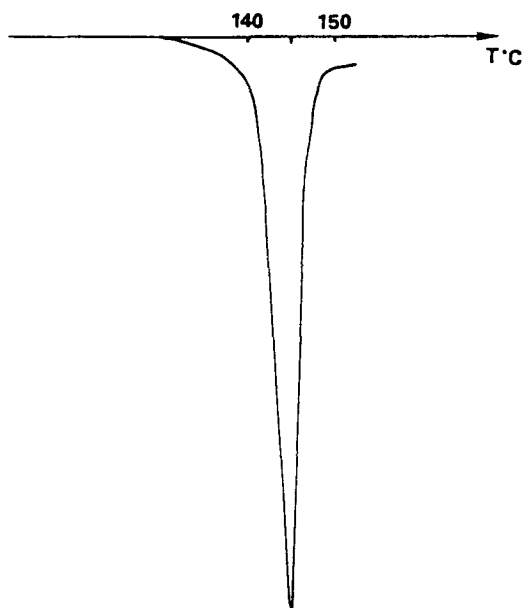
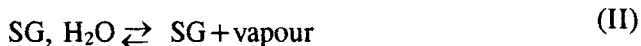


Fig. 2 DTA curve of the sulfaguanidine monohydrate in sealed tube (heat rate: 1 deg·min<sup>-1</sup>)

rium II between hydrate, anhydrous compound and vapour, immediately took place:

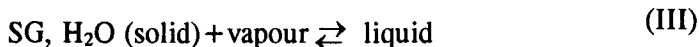


where the forward reaction takes place when temperature rises.

The vapour spread in the dead volume, and since the vapour pressures of the solid anhydrous and hydrate forms are low, we can assume that it contained almost only water. Hence, in each tube, there was a vapour pressure which varied as a function of temperature.

During heating, the hydrate partially lost water vapour. The pure monohydrate gave rise to a mixture of three phases: the solid monohydrate, the solid anhydrous form and the vapour phase.

2) If the endotherm observed corresponds to the congruent melting of the hydrate form, in a closed vessel, it must represent the triple point:



As a matter of fact, the presence of the anhydrous form made the phenomenon more complex. It can be explained with the help of a 'temperature-specific volume-molar fraction' ( $T$ - $V/m$ - $x$ ) diagram [4].

### Isochoric polythermal study

The MCB ARION microcalorimeter was used. The samples were prepared by mixing either anhydrous sulfaguanidine with monohydrate, or monohydrate with water. The volume of the vessels and the mass of the samples were such that the  $V/m$  ratio varied approximately between 3.5 and 5.5  $\text{mm}^3 \cdot \text{mg}^{-1}$ .

The polythermal diagram which is presented in Fig. 3 was obtained with 0.5 and 1.0  $\text{deg} \cdot \text{min}^{-1}$  heating rates.

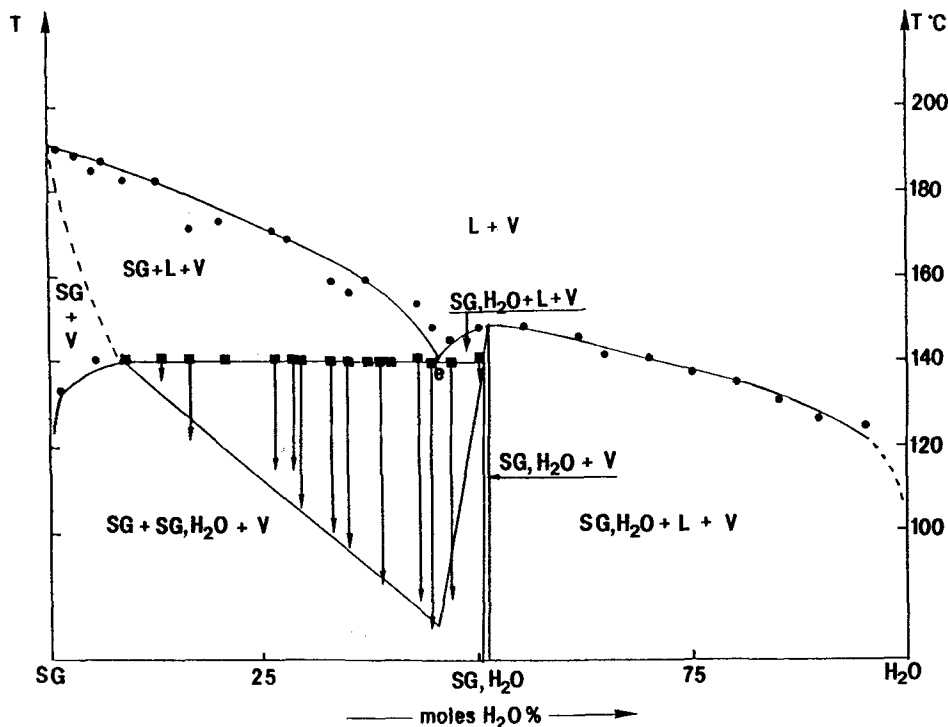


Fig. 3 Sulfaguanidine-water system. Isochoric section:  $3.5 < v < 5.5 \text{ mm}^3 \cdot \text{mg}^{-1}$

A horizontal invariant line can be observed at  $141^\circ\text{C}$ , between anhydrous sulfaguanidine and monohydrate. It must be noticed that for the composition of the monohydrate, the DTA peak observed (Fig. 2) has a liquid shape (with a top temperature at  $148^\circ\text{C}$ ). In principle, this peak should have the shape of a pure compound melting, since the composition is that of the pure monohydrate. Furthermore, in Fig. 3, it can be observed on the liquidus curve between the monohydrate and the anhydrous form, that there is a strong possibility of the existence of an eutectic point between 40 and 50 mol  $\text{H}_2\text{O}$  %. Nevertheless, regarding the DSC endotherms, it is not even possible to eliminate definitely the case of a degenerated peritaxy at the monohydrate composition. The Tammann

diagram is not sufficient to let us take a definite position about the question since the liquidus and invariant peaks cannot be separated in the monohydrate region. But the temperature of the liquidus curve in the monohydrate ( $T \approx 148^\circ\text{C}$ ) indicates that there is no degenerated peritectic since the invariant temperature which occurs between anhydrous sulfaguanidine ( $SG$ ) and monohydrate ( $SG, \text{H}_2\text{O}$ ) is  $141^\circ\text{C}$ . On another hand, the maximum of the liquidus curve is not observed for  $x_{\text{H}_2\text{O}} = 0.5$  but for  $0.50 < x_{\text{H}_2\text{O}} < 0.55$ .

Though the DTA curves are not quite perfect, the diagram of the region laying between  $SG, \text{H}_2\text{O}$  and  $\text{H}_2\text{O}$  can be more easily interpreted. This region of the diagram is characterized by a liquidus with a light inflexion in its central part. The liquidus curve falls to an eutectic line which has not been detected because it occurs at a temperature lower than  $0^\circ\text{C}$  (melting point of water).

## ***T-V/m-x representation***

### *a) The monohydrate behaviour*

It is shown in Fig. 1 that the monohydrate undergoes a non negligible pressure dissociation. For this reason, in the present experimental conditions, solid-liquid equilibria could not be observed in the absence of a vapour phase.

After fast cooling of a sulfaguanidine monohydrate sample which had first been annealed during four days at  $130^\circ\text{C}$  (i.e. a few degrees beyond the melting point) in a sealed pyrex tube, drops of liquid were observed on the tube wall. This liquid formed during cooling, by condensation of the vapour phase which coexisted at  $130^\circ\text{C}$  in equilibrium with the two solid phases (hydrate and anhydrous forms). The analysis of the liquid by spectrophotometric method at 265 nm showed that the sulfaguanidine molar fraction was about 0.03 ( $x_{\text{H}_2\text{O}} = 0.97$ ).

In the following sections, we will demonstrate that, at  $130^\circ\text{C}$ , for the composition  $x_{\text{H}_2\text{O}} = x_{\text{SG}} = 0.5$ , equal to that of the monohydrate, and for a specific volume  $V/m = 4 \text{ mm}^3 \cdot \text{mg}^{-1}$ , a three phase equilibrium takes place between  $SG, SG, \text{H}_2\text{O}$  and a vapour phase. In these conditions we may assume that the vapour composition is nearly the same as that of the vapour at eutectic equilibrium ( $141^\circ\text{C}$ ).

### *b) Theoretical aspect of temperature-specific volume-molar fraction (T-v-x) diagrams*

When the thermal effects recorded by thermal analysis are attributed to the equilibria which occur among condensed phases, the study of systems with non negligible vapour pressure can be performed by two different ways:

- the dead volume is nul and there is no vapour phase,
- the loss of matter by vaporization can be calculated at all temperatures for the different compositions.

In the present work, thermal effects have been related to the following parameters:

- the internal volume  $V$  of the tube (i.e. the total volume of heterogeneous sample including vapour),
- the total mass of the sample  $m$ ,
- the molar fraction of water.

The theoretical  $T$ - $v$ - $x$  diagram (where  $v=V/m$ ) for systems containing one hydrate has been presented in a recent paper [1] which is a continuation of our previous work on metal-arsenic systems [4-7].

It must be reminded that the vapour in equilibrium with condensed phases is always rich in water (more volatile constituent) and that the specific volume of a vapour phase is much greater than that of the condensed phases. In the  $T$ - $v$ - $x$  diagram, four phases coexist at the invariant equilibrium. Each of these phases is characterized by its own composition and its own specific volume. Thus, the graphic representation of the invariant equilibrium is either a quadrilateral or a triangle.

In this kind of diagram, as well as in the classical temperature-molar fraction ( $T$ - $x$ ) diagram where pressure is supposed to be constant, a binary compound with congruent melting divides the system into two subsystems. Thus, sulfaguanidine monohydrate separates the sulfaguanidine-water system into two subsystems.

In the case of such systems with a hydrate form, the eutectic plane of the water-rich end must be quadrilateral, since, at the triple point, the specific volume of liquid water is smaller than the specific volume of ice. On the contrary, in the water-poor end of the diagram, the eutectic plane is a triangle.

Nethertheless, it must be pointed out that the graphic representation of the three phase equilibrium at the congruent melting point of a binary compound, heated in a tube of constant volume, is a straight line joining the three representative points of the solid, liquid and vapour phases. This is the only condition imposed, in  $T$ - $v$ - $x$  diagrams, for the congruent melting. Thus, the compositions of the three phases are not necessarily equal.

### *c) Determination of the limits of the invariant plane of the subsystem SG-SG, H<sub>2</sub>O*

The endotherms which occur on DTA curves can easily be explained by the use of the  $T$ - $v$ - $x$  diagram, but it has not been possible to draw the invariant planes with an as accurate precision as that obtained in our previous works on mineral systems. This is indeed in relation with the experimental problems caused by the presence of water which creates vapour and liquid flows in the tube.

Four isoplethal sections have been studied corresponding to the following water molar fractions: 0.10, 0.20, 0.37 and 0.50. The experimental results must let us draw the limits of the invariant plane. The method consists in plotting a Tammann diagram for each isoplethal curve. For each composition, the thermal effect of the invariant equilibrium becomes nul when the limit of the invariant plane is reached. Thus, the *SG*-vapour side of the invariant plane can be drawn.

If the invariant equilibrium is an eutectic invariant, the tie-line joining the eutectic point  $L_e$  and the vapour point  $V$  at the eutectic equilibrium can easily be drawn, since this tie-line corresponds to the maximum thermal effect. Moreover, this line must intercept the isoplethal section  $x_{(H_2O)}=0.5$ . This is not possible in the case of a peritectic equilibrium. In this case, the maximum thermal effect corresponds to a tie-line *SG*,  $H_2O$ -vapour which is not visible at the composition  $x_{(H_2O)}=0.5$ .

The Tammann diagrams obtained are presented in Figs 4–7. The uncertainty on the extrapolation for  $S/m=0$  (where  $S/m$  is the surface of peak per mass unit)

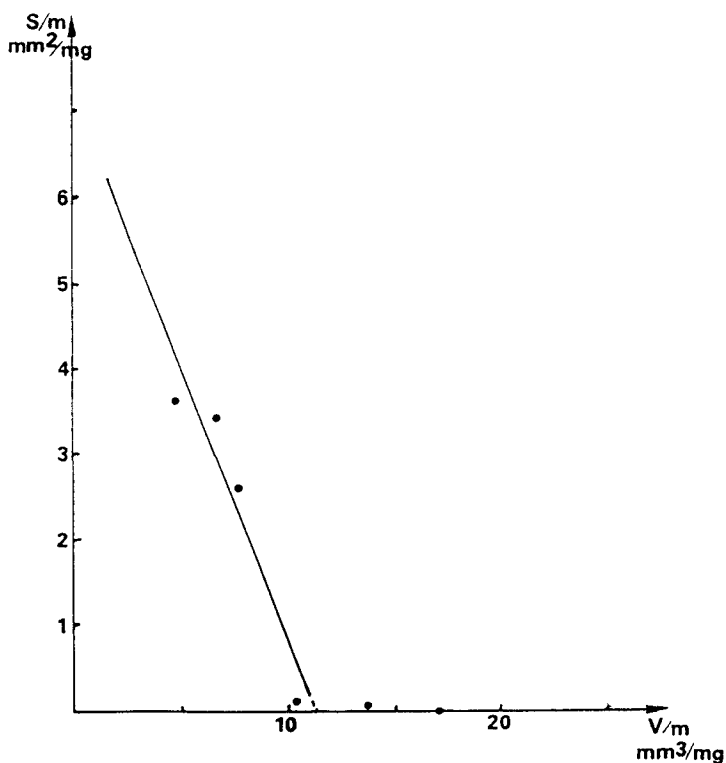


Fig. 4 Isoplethal section  $x_{H_2O}=0.1$ . Surface of invariant peak/sample mass vs. specific volume:  $S/m=f(v)$  at  $T=141^\circ\text{C}$



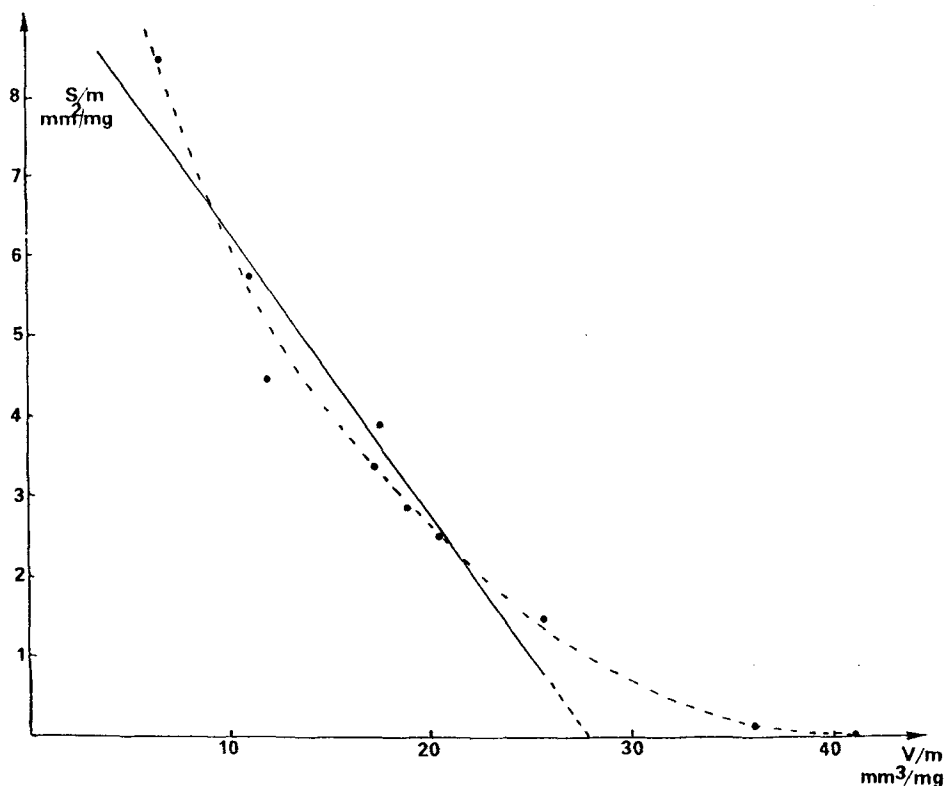


Fig. 5 Isolethal section  $x_{\text{H}_2\text{O}}=0.2$ . Surface of invariant peak/sample mass vs. specific volume:  $S/m=f(v)$  at  $T=141^\circ\text{C}$

made us take into account two  $S/m$  values for each composition. The lowest value, is obtained by drawing a straight line passing through the points average; then, for each composition, the  $V/m$  value obtained for  $S/m=0$ , corresponds to the limit of the invariant. The highest value is obtained by drawing a curved line which is extrapolated for  $S/m=0$ . These two series of data have been reported in the  $x-V/m$  plane (Fig. 8).

The alignment of the points obtained from the four Tammann diagrams indicates the direction of the  $SG$ -vapour side ( $SG-V$ ) of the invariant triangle.

At  $130^\circ$ , the experimental molar fraction of the water in the vapour is  $x_{\text{H}_2\text{O}}=0.97$ . It must be noticed that, by continuing the straight line  $SG$ -vapour up to this value, the specific volume of the vapour is included between 170 and  $200 \text{ mm}^3 \cdot \text{mg}^{-1}$ . This will be nearly the specific volume of the vapour phase at the invariant equilibrium (point  $V$  in Fig. 8) if the change in composition between 130 and  $141^\circ\text{C}$  is negligible.

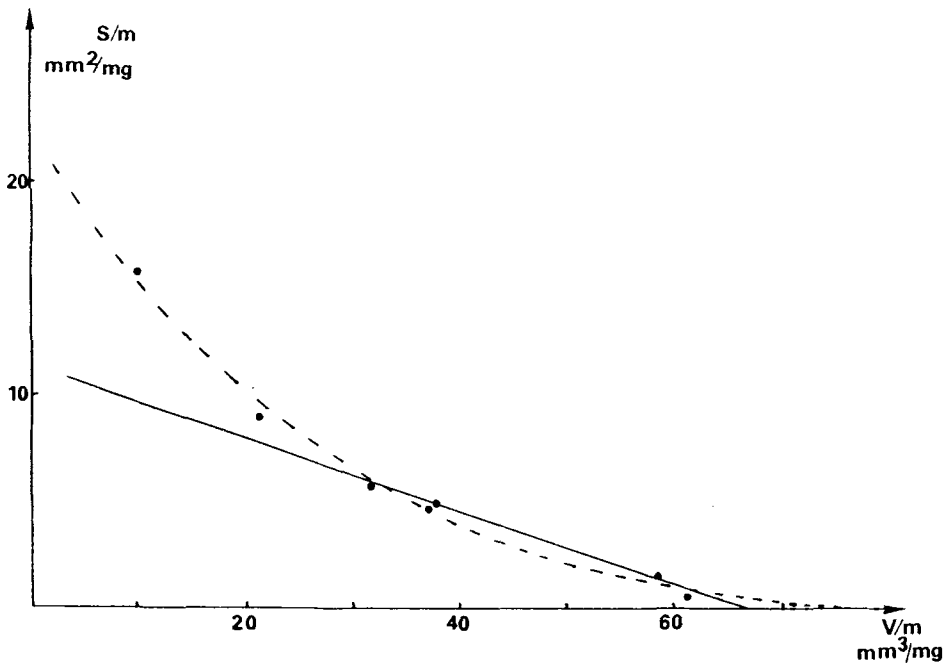


Fig. 6 Isolethal section  $x_{\text{H}_2\text{O}}=0.37$ . Surface of invariant peak/sample mass vs. specific volume:  $S/m=f(v)$  at  $T=141^\circ\text{C}$

*d) Liquid  $L_e$ -vapour tie-line on the eutectic plane*

The isoplethal section drawn for  $x_{\text{H}_2\text{O}}=0.5$  gives us some more information about the eutectic liquid-vapour tie-line. We have earlier indicated that the interpretation of the DTA curves was difficult because of the superposition of the eutectic peak with the liquidus curve. At first sight, it seems impossible to draw a Tammann diagram with such endotherms (Fig. 9). This is why we measured the total endotherm surface (invariant+liquidus) when it was impossible to measure the only invariant endotherm. The results are reported in Fig. 7.

The results obtained with 36 samples (Fig. 7) indicate the existence of a break of the slope of the  $S/m=f(V/m)$  curve for  $V/m=28.5 \text{ mm}^3 \cdot \text{mg}^{-1}$  (point C). In the case of an eutectic triangle, the liquidus must disappear for the value of  $V/m$  which corresponds to the intersection of the isoplethal section  $x=0.5$  with the eutectic liquid-vapour ( $L_e$ - $V$ ) tie-line (Fig. 8). At this point, the thermal effect at the invariant equilibrium must be maximum. Thus, this point must be point C (Fig. 7). For  $V/m < 28.5 \text{ mm}^3 \cdot \text{mg}^{-1}$ , the endotherms represent both liquidus and eutectic effects. For  $V/m > 28.5 \text{ mm}^3 \cdot \text{mg}^{-1}$ , the endotherms are only due to the eutectic equilibrium. Point C corresponds to the maximum eutectic thermal effect. Furthermore, the distribution of the liquidus temperatures on the isoplethal section (Fig. 10) shows the existence of an eutectic liquid-vapour valley.

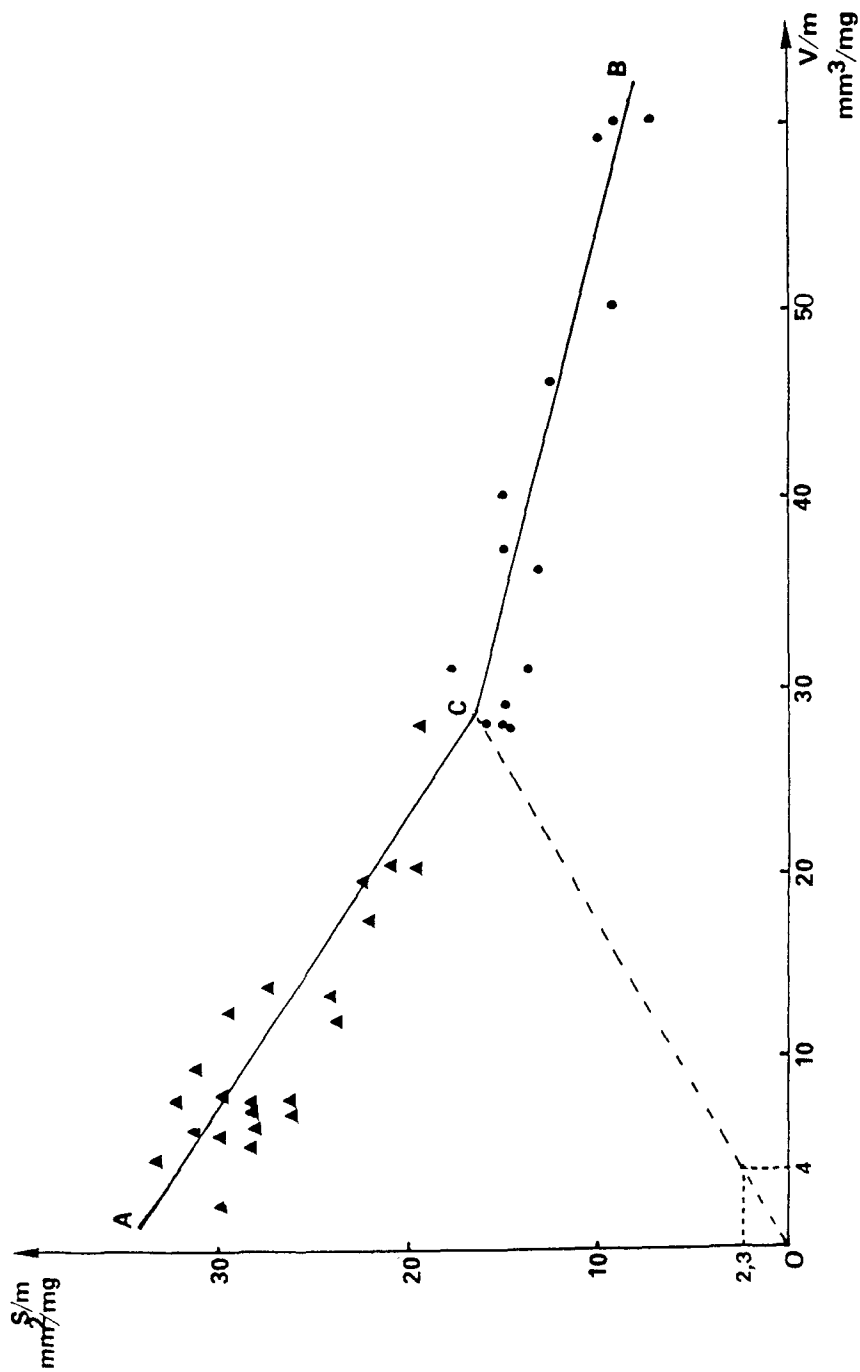


Fig. 7 Isothermal section  $x_{H_2O} = 0.5$ . Surface of invariant peak/sample mass vs. specific volume:  $S/m = f(v)$  at  $T = 141^\circ C$ ;  $\blacktriangle$  Total surface (invariant peak + liquidus peak);  $\bullet$  Surface of invariant peak

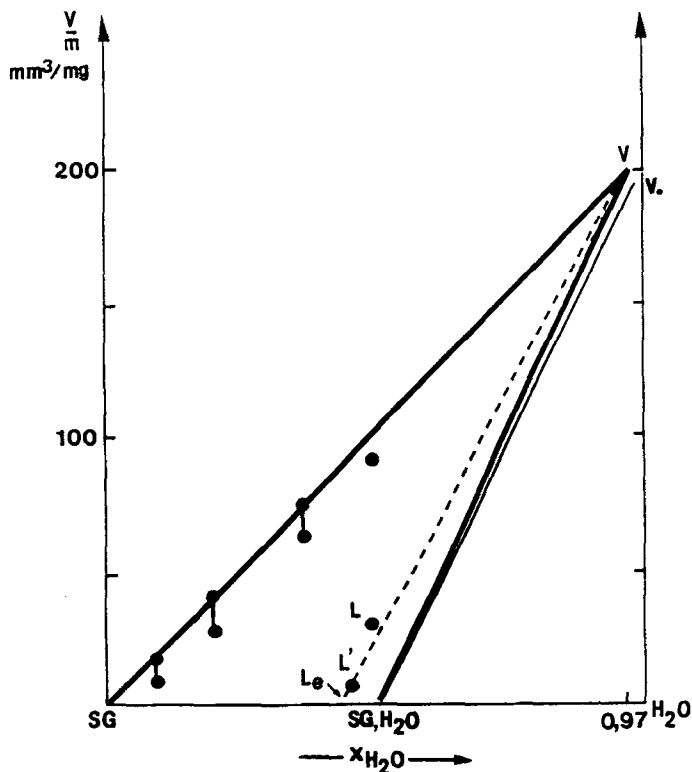


Fig. 8 Eutectic invariant in the  $x-v$  plane

Thus, the eutectic liquid-vapour ( $L_e-V$ ) tie-line passes through the point  $L$  ( $x_{H_2O}=0.5$ ,  $V/m=28.5$   $\text{mm}^3\cdot\text{mg}^{-1}$ ) (Fig. 9). This is the proof that the invariant is an eutectic invariant and not a peritectic invariant.

On another hand, in Fig. 7, the rising part of the Tammann diagram for  $x_{H_2O}=0.5$  has been drawn by joining the axis origine to point  $C$ . On this curve, the  $S/m$  value has been determined for  $V/m \approx 4$   $\text{mm}^3\cdot\text{mg}^{-1}$ :  $S/m=2.3$   $\text{mm}^2/\text{mg}^{-1}$ . Then, this value has been used on the Tammann diagram of the isochoric section obtained for  $V/m \approx 4$   $\text{mm}^3\cdot\text{mg}^{-1}$  (Fig. 3). This makes the determination of the eutectic point more precise on this section. The molar fraction is  $x_{H_2O}=0.45$  for the eutectic point in the section  $V/m \approx 4$   $\text{mm}^3\cdot\text{mg}^{-1}$  (point  $e$  of Fig. 3 and point  $L'$  of Fig. 8). The molar fraction of the eutectic point in the triangle  $SG-V-SG$ ,  $H_2O$  must not be very different from this value (point  $L_e$  of Fig. 8).

#### *e) Determination of the coordinates ( $x$ , $V/m$ ) of the vapour phase at the eutectic equilibrium*

The coordinates of the point representing the vapour phase at the eutectic equilibrium must be determined by the intersection of the two straight lines

$SG$ -vapour and eutectic liquid-vapour. However, the two points  $L$  ( $x_{H_2O}=0.5$ ,  $V/m=28.5$ ) and  $L'$  ( $x_{H_2O}=0.45$ ,  $V/m=4$ ) are not sufficient for drawing the straight line  $L_e$ -vapour with a good accuracy.

The water experimental molar fraction at  $130^\circ\text{C}$ , is  $x=0.97$ . This value must be very close to that of water molar fraction at  $141^\circ\text{C}$ . Thus, the point  $V$  obtained for  $x_{H_2O}=0.97$  on the  $SG$ -vapour straight line of the eutectic plane, represents the vapour phase at the eutectic equilibrium. Then, the tie-line  $L_e$ - $V$  passes through  $L'$ ,  $L$  and  $V$ .

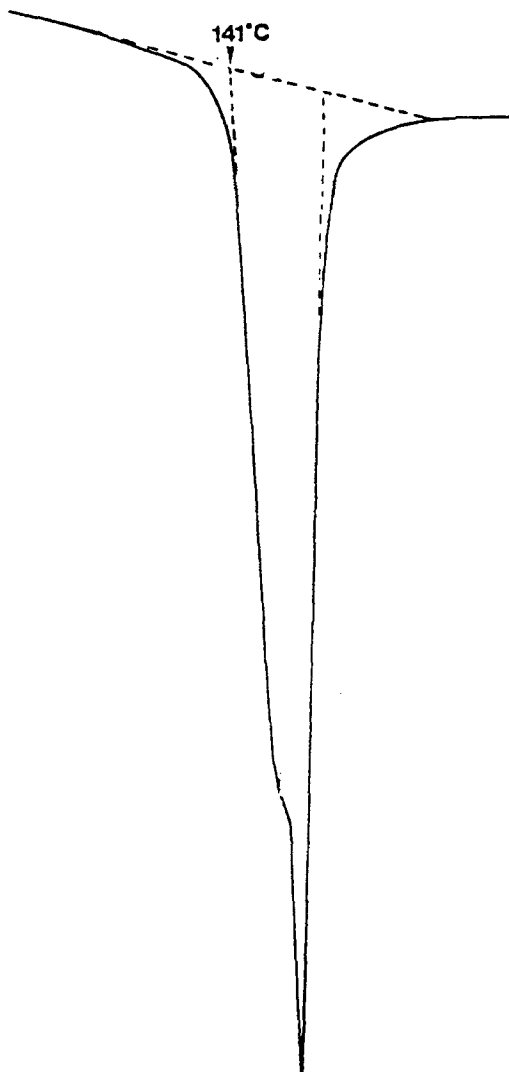


Fig. 9 Superposition of the invariant and liquidus peak.  $V/m=7.0 \text{ mm}^3 \cdot \text{mg}^{-1}$ . Heating rate  $=0.5 \text{ deg} \cdot \text{min}^{-1}$ .

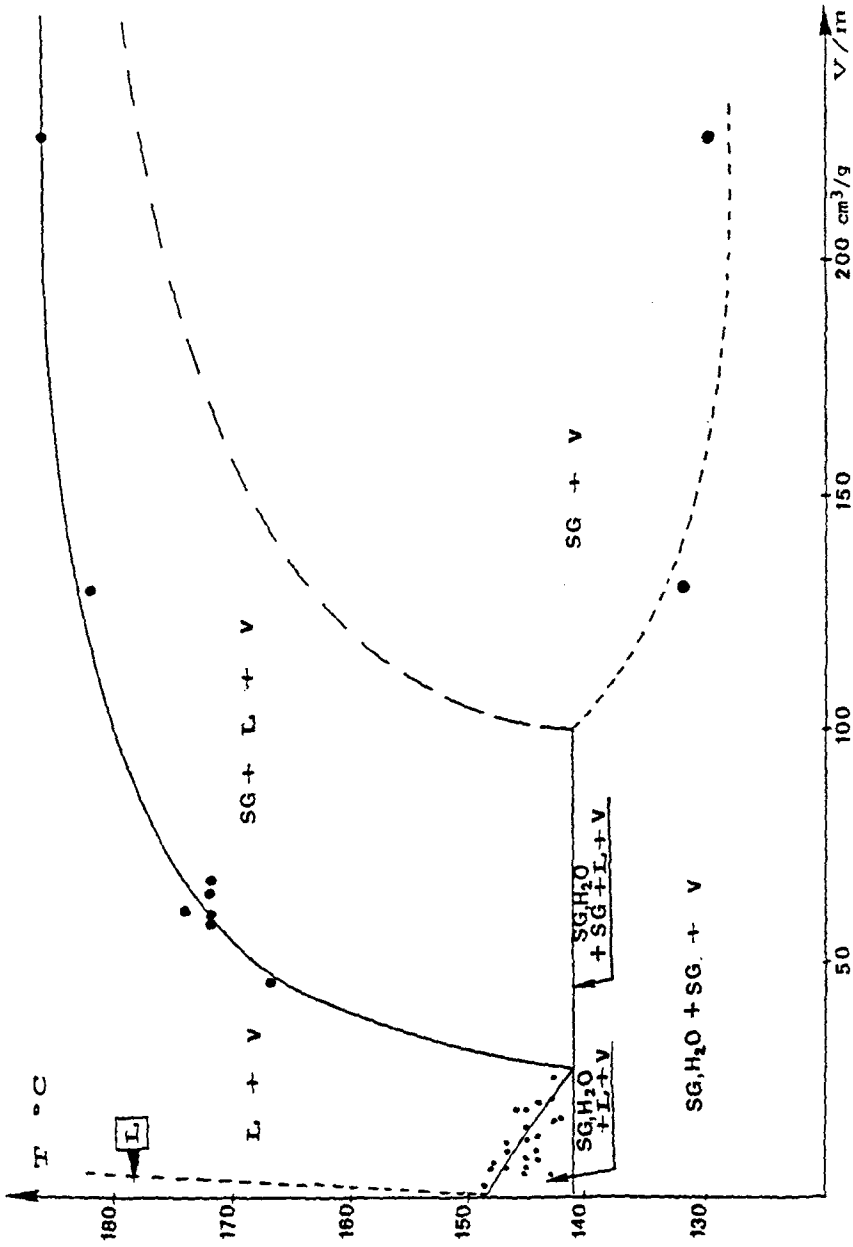


Fig. 10 Isoplethal section:  $x_{\text{H}_2\text{O}} = 0.1$

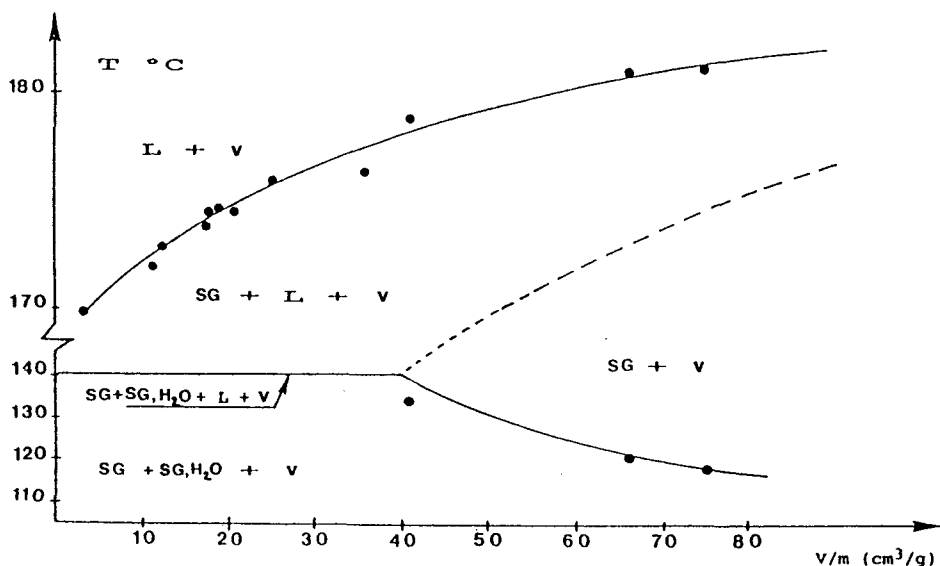
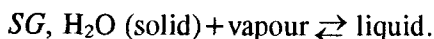


Fig. 11 Isolethal section:  $x_{H_2O}=0.2$

On the straight lines  $SG-V$ , the molar fraction  $x=0.97$  corresponds to  $V/m=200 \text{ mm}^3 \cdot \text{mg}^{-1}$ .

The line  $SG, H_2O-V_0$  (where  $V_0$  must have almost the same coordinates as point  $V$ ) figures the triple line relating the congruent melting of monohydrate  $SG, H_2O$  at  $148^\circ\text{C}$ :



The isoplethal sections of Figs 11 to 12 show that the experimental liquidus curves are consistent with those of the theoretical sections [1]. These sections are also consistent with the determination of the invariant plane with the Tamman diagrams presented in Figs 4 to 6. They also lead to the  $SG-SG, H_2O-V$  eutectic plane which is drawn in Fig. 8.

## Conclusions

The experimental study of this system has been made difficult for two reasons. First, it was not easy to prepare samples of strictly constant compositions for variable specific volumes. Second, there was, in the tubes, a temperature gradient which lead to flow phenomenons and which made the samples heterogeneous.

Nevertheless, it has been assessed that the three-dimension system was divided into two sub-systems by the pure hydrate phase diagram. In this diagram, an invariant line at  $148^\circ\text{C}$  relates the equilibrium

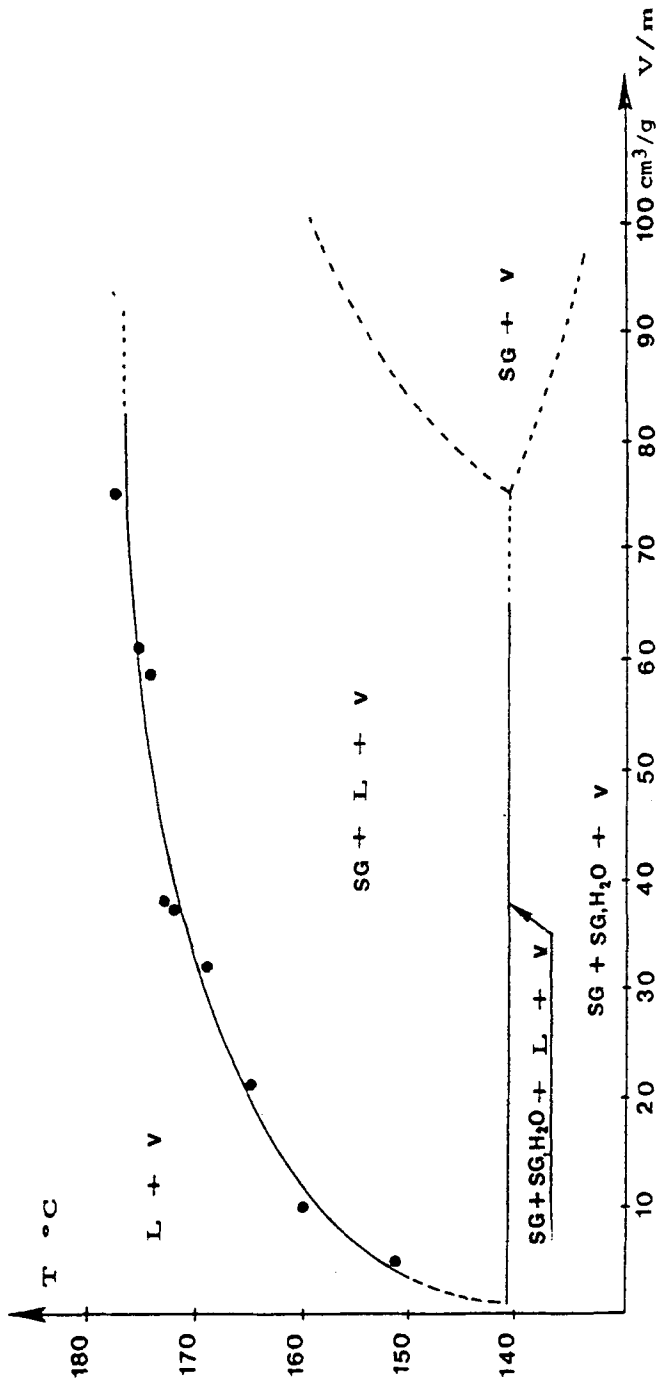


Fig. 12 Isoplethal section:  $x_{H_2O} = 0.37$



$SG, H_2O$  solid + vapour  $\rightleftharpoons$  liquid

We have demonstrated that the invariant plane of the anhydrous sulfaguanidine-rich end was an eutectic plane and that the melting of sulfaguanidine monohydrate was a congruent melting.

We have also demonstrated that the triple line of the pure hydrate phase diagram could not be perpendicular to the composition axis. Then, the three phases in equilibrium (solid, liquid, vapour) must have different compositions. This is consistent with the DTA results obtained for pure sulfaguanidine and with the position of the maximum of the liquidus curve which deviates slightly from the stoichiometric composition of  $SG, H_2O$ , as it has been observed on the isochoric section.

## References

- 1 J. C. Rouland, S. A. Thorén, J. L. Fournival and R. Céolin, *J. Thermal Anal.* (1995) in press.
- 2 S. Alberola, J. Rambaud, F. Sabon, *Bulletin de la Société Chimique de France*, 3-4 (1977) 181.
- 3 G. Thévenet, Thesis, University Paris-Sud, 1980, p. 4.
- 4 J. C. Rouland, Thesis, University Paris-Sud, 1983.
- 5 J. C. Rouland, C. Souleau and R. Céolin, *J. Thermal Anal.*, 30 (1985) 429.
- 6 J. C. Rouland, C. Souleau and R. Céolin, *J. Thermal Anal.*, 30 (1985) 1077.
- 7 J. C. Rouland, C. Souleau and R. Céolin, *J. Thermal Anal.*, 31 (1986) 305.

**Zusammenfassung** — Das System Sulfaguanidin-Wasser ( $SG-H_2O$ ) ist ein binäres System mit einem nicht unwesentlichen Dampfdruck und liefert ein Monohydrat. Das Phasendiagramm dieses Systemes wurde anhand der experimentellen DTA-Ergebnisse konstruiert, dabei kam das in Teil I vorliegender Arbeit beschriebene Temperatur-spezifisches Volumen-Molenbruch ( $T-v-x$ ) zur Anwendung.

Das Monohydrat ( $SG, H_2O$ ) schmilzt kongruent. Es werden isochore Bereiche gezeichnet, die eine Bestimmung der Grenzen der zwei eutektischen invarianten Flächen ermöglichen. Es werden Zusammensetzung und spezifisches Volumen der Dampfphase im eutektischen Gleichgewicht des Untersystemes  $SG-SG, H_2O$  angegeben. Die Tripel-Linie (solidus-liquidus-vapourus) des Einkomponenten-Phasendiagrammes des Monohydrates wird gezeichnet. Die experimentellen Ergebnisse stimmen mit dem kongruenten Schmelzen des Monohydrates überein. Diese Ergebnisse zeigen weiterhin, daß die Feststoff-, die Flüssigkeits- und die Dampfphase an der Tripel-Linie nicht die gleiche Zusammensetzung besitzen.